

Explicit global simulation of the mesoscale spectrum of atmospheric motions

Yoshiyuki O. Takahashi,¹ Kevin Hamilton,² and Wataru Ohfuchi³

Received 27 March 2006; revised 9 May 2006; accepted 22 May 2006; published 27 June 2006.

[1] The horizontal spectrum of kinetic energy in the upper troposphere in experiments conducted with the Atmospheric GCM for the Earth Simulator (AFES) global spectral general circulation model is examined. We find that the control version of AFES run at T639 spectral resolution can simulate a realistic kinetic energy spectrum with roughly -3 power-law dependence on horizontal wavenumber for wavelengths between about 5000 and 500 km, transitioning to a shallower mesoscale regime at smaller wavelengths. The results depend to a degree on the magnitude of the parameterized horizontal hyperdiffusion, but the existence of a distinct shallow mesoscale range in the simulations is independent of the hyperdiffusion employed. We present results from a number of AFES integrations with spectral truncations ranging from T39 to T639 and determine the appropriate scaling of the parametrized hyperdiffusion with model numerical resolution so that the kinetic energy spectrum in each case converges to realistic values. The experiment was also repeated in a dry version of the model. This version also simulated a shallow mesoscale range, supporting the view that the mesoscale regime in the atmosphere is energized, at least in part, by a predominantly downscale nonlinear spectral cascade. **Citation:** Takahashi, Y. O., K. Hamilton, and W. Ohfuchi (2006), Explicit global simulation of the mesoscale spectrum of atmospheric motions, *Geophys. Res. Lett.*, 33, L12812, doi:10.1029/2006GL026429.

1. Introduction

[2] The spectrum of wind velocity variance as a function of horizontal scale in the atmosphere is often referred to as the kinetic energy (KE) spectrum. *Boer and Shepherd* [1983] used global gridded meteorological analyses to calculate the horizontal KE spectrum as a function of total horizontal wavenumber, n . They found that the KE behaves as n^{-3} for the range of n corresponding to horizontal wavelengths between 1000 and 5000 km. For horizontal wavelengths smaller than ~ 1000 km, perhaps the best observations come from measurements of the winds in the upper troposphere using instrumented commercial aircraft [*Nastrom and Gage*, 1985]. The crosses on the two panels of Figure 1 reproduce the observations for the zonal and meridional velocity variance as a function of horizontal wavelength based on long segments of aircraft flights

mostly in the northern midlatitudes, and between 175 and 350 hPa. There is a transition from a -3 power law to a shallower mesoscale regime at wavelengths less than about 500 km. More recent analyses of other extensive aircraft data sets confirm this basic result [*Cho et al.*, 1999a, 1999b].

[3] The -3 power law regime has been interpreted as resulting basically from the weak forward spectral cascade of kinetic energy from a quasi-2D flow that is effectively stirred at synoptic scales by baroclinic instability. The explanation for the much shallower spectrum in the mesoscale is more controversial. Some [e.g., *Lilly*, 1983; *Gage and Nastrom*, 1986; *Vallis et al.*, 1997] suggest that the energized mesoscale results from an upscale quasi-2D nonlinear KE cascade from smaller scales where the KE is stirred by moist convection. Alternatively the motions in the mesoscale range may be forced by downscale nonlinear cascades possible in systems that allow gravity-wave type divergent motions [e.g., *VanZandt*, 1982]. Support for this latter view is provided by some simplified models of turbulence in systems including free gravity waves [*Yuan and Hamilton*, 1994] and also by the observational analysis of *Lindborg* [1999].

[4] The horizontal KE spectrum has been examined in a number of earlier studies using relatively modest horizontal resolution GCMs [*Boville*, 1991; *Koshyk et al.*, 1999]. These studies showed that GCMs can reproduce a realistic n^{-3} regime in the troposphere but, due to the limited horizontal resolution, these models did not allow simulation of a significant range of the shallower mesoscale regime.

[5] It appears that various current high-resolution GCMs perform rather differently in terms of their ability to simulate a realistically shallow mesoscale kinetic energy spectrum. *Palmer* [2001] notes that the ECMWF GCM, when run at fine resolution, actually simulates flow with a KE spectrum that steepens rather than shallows in the mesoscale. As he notes, if this is a general feature of current models - which assume that an important component of subgrid-scale processes can be parameterized as a viscous dissipation acting on the smallest resolved scales - then it would suggest that some kind of stochastic forcing of the smallest resolved scales may be more appropriate than the usual dissipation. However, *Koshyk and Hamilton* [2001, hereinafter referred to as KH] found that a GCM with standard subgrid-scale dissipation can simulate a realistically energized mesoscale. In particular, KH analyzed results from a control simulation with a ~ 35 km horizontal resolution, 40-level version of the SKYHI GCM. KH found that their simulated fields did reproduce the shallow one-dimensional horizontal KE spectra observed by *Nastrom et al.* in the upper troposphere down to the smallest model-resolved wavelength (~ 70 km). KH resolved their

¹Graduate School of Science, Hokkaido University, Sapporo, Japan.

²International Pacific Research Center, University of Hawaii, Honolulu, Hawaii, USA.

³Earth Simulator Center, Japan Agency for Marine-Earth Science and Technology, Yokohama, Japan.

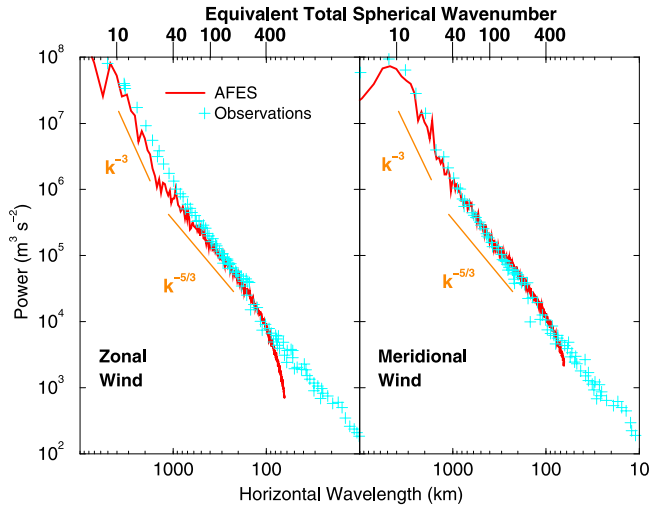


Figure 1. The one-dimensional horizontal power spectra of (left) zonal wind and (right) meridional wind variations near the tropopause. The red curves are computed from wind values taken along the 45N latitude circle at 200 hPa in the T639L24 AFES. The crosses are from *Nastrom and Gage* [1985] and are computed from wind observations taken by commercial airliners. Orange lines show -3 and $-5/3$ slopes.

simulated flow into spherical harmonics and computed 2D spectra as a function of total wavenumber n . This also displays the transition from $\sim n^{-3}$ to a shallower ($\sim n^{-5/3}$) mesoscale range starting near $n \sim 80$ (corresponding to horizontal wavelengths of about 500 km). KH performed some detailed diagnostics that indicated that the mesoscales are significantly energized by both downscale nonlinear spectral cascades and a conversion (local in spectral space) from available potential energy to KE.

[6] KH presented only results from a single control run and are thus limited to the specific model formulation in the standard SKYHI code. The SKYHI model is somewhat unusual in its numerical formulation relative to most other current global atmospheric GCMs. Of particular concern is the SKYHI model grid-point approximation of the governing equations using simple second-order Eulerian differences on a non-staggered horizontal grid, which may possibly cause an artificial buildup of enstrophy and energy at small scales [Arakawa, 1966]. The second point of concern is that the SKYHI model has only been run with convective processes parameterized by moist convective adjustment (MCA). The use of MCA in GCMs has been found to lead to simulation of possibly unrealistically noisy tropical precipitation fields which might act as an artificially enhanced forcing of mesoscale motions.

2. AFES Model

[7] The AFES model was adapted from the CCSR/NIES AGCM [e.g., Numaguti *et al.*, 1997] to run efficiently on the Earth Simulator [Ohfuchi *et al.*, 2004]. The version employed here is a spectral GCM with standard semi-implicit time-marching formulation and spectral advection scheme. A fourth-order horizontal subgrid-scale hyperdiffu-

sion is employed in the momentum, thermodynamic and water vapor and cloud water equations. The model can be run with several different moist convective parameterization schemes, but all the results shown here were obtained employing the Emanuel scheme [e.g., Emanuel, 1991]. We will discuss results from a number of experiments with T639L24 and T639L48 versions along with some lower resolution versions. The top model level is located at roughly 1 hPa. Each experiment lasts 15 days and begins from an initial condition interpolated from the end of a long control run with a T319L24 version of the model. The initial conditions for the present standard control run are for June 1 and ocean surface temperatures are prescribed to climatological values.

3. Results for the KE Spectrum

[8] The solid curves in Figure 1 show the one-dimensional variance spectra of zonal and meridional wind at 200 hPa around the 45N latitude circle, computed from hourly snapshots during days 6–15 of the T639L24 simulation. These are shown with the comparable observations. It is apparent that the model simulates quite realistic 1D wind variance spectra over much of the shallow mesoscale regime, although there is an unrealistic steepening near the end of the simulated spectra. Note the spectra are shown out to the wavenumber traditionally regarded as corresponding to the 2D truncation, i.e., $1/l_T$ in the notation of *Lander and Hoskins* [1997]. However, Lander and Hoskins show that the physical space results reconstructed from a spectral model representation do not adequately capture straightline spatial variations down to wavenumbers of $1/l_T$, and they would regard the results of a 1D spectrum between wavenumbers $1/(2^{1/2}l_T)$ and $1/l_T$

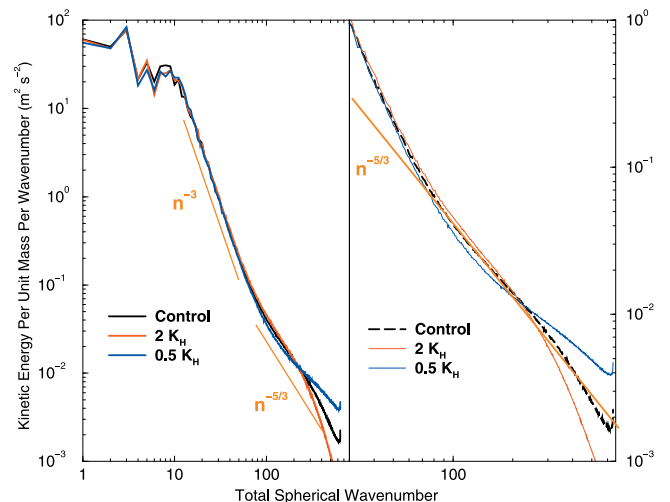


Figure 2. Kinetic energy per unit mass on the 200 hPa surface in the AFES model as a function of the total spherical harmonic wavenumber. Results from the T639L24 AFES model when run with different values of the horizontal diffusion coefficient: the standard value (black), twice the standard value (red) and one-half the standard value (blue). The right panel is a blowup of the results for the wavenumber 30 through 639 range. Orange lines show -3 and $-5/3$ slopes for comparison.

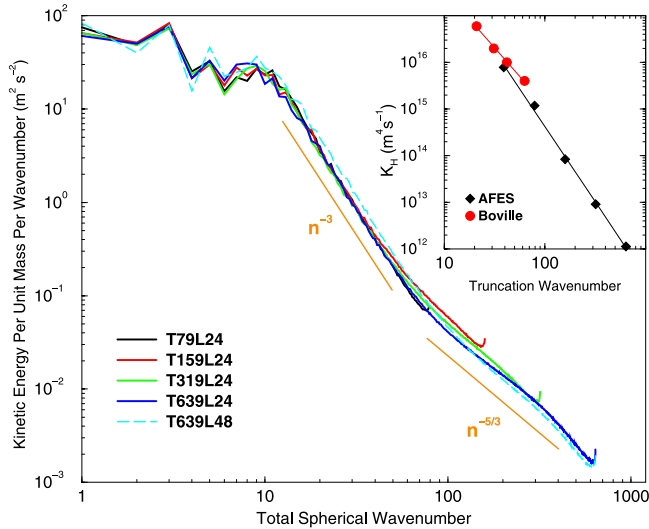


Figure 3. As in Figure 2 but for AFES run with different numerical resolution. Results are shown for the 24 level version truncated at T79, T159, T319 and T639, as well as the T639L48 version. At each horizontal resolution a diffusion coefficient has been determined by trial and error to produce the fairly convergent behavior at the high wavenumber end of the spectrum. The black symbols in the inset show the diffusion coefficient as a function of the truncation obtained this way. The red dots show results from a similar analysis of a version of the NCAR atmospheric model obtained by *Boville* [1991]. The lines in the inset are linear regressions.

as not believable. Indeed we find that the steepening near the end of the spectrum in Figure 1 has no counterpart in the full 2D spectrum. Figure 2 shows this 2D total horizontal wavenumber KE spectrum at 200 hPa calculated from the simulated vorticity and divergence fields (equation (6) of KH). The left panel shows results for the full range of wavenumbers resolved (1–639) and the right panel shows a closeup of the 30–639 range. Results are presented for the simulations with the control value of the hyperdiffusion coefficient and with twice and one-half this value. The result with the control value of diffusivity displays a mesoscale regime that is close to a constant slope over much of the mesoscale, although there is a slight bending down past $n \sim 300$ and an abrupt increase at the highest few wavenumbers. The anomaly right near the truncation wavenumber is a feature of the simulated spectra in this model at all resolutions. The appearance of this feature suggests that the nonlinear interactions in the model are resulting in a forward cascade of energy that is arrested at the truncation scale and accumulates there. This is a feature of many numerical simulations and may be eliminated with an appropriately scale-dependent dissipation. Fortunately, in this case the apparently anomalous values are confined to just a few wavenumbers.

[9] The model when run with the enhanced and reduced diffusivity coefficients is much less successful in simulating the observed constant slope of the mesoscale spectrum. It is noteworthy that the doubled standard diffusivity run (red curves) appears to be overdamped over most of the high

wavenumber end of the spectrum, but still exhibits a clear shallowing of the spectrum in the mesoscale range, from say $n \sim 80$ to $n \sim 250$.

4. Resolution Dependence and Scaling of Parameterized Diffusion

[10] A series of simulations with different truncations (from T39 to T639) and different values of the horizontal diffusivity were run. By trial and error choices of the diffusivity, the result in Figure 3 was obtained. This shows simulated spectra that are nearly independent of the truncation over the n^{-3} and shallower mesoscale regimes (for legibility the T39 result is not shown but it agrees well with the others). The values of the diffusivity used in each of these experiments is shown in the upper right panel. We find that to obtain the convergent spectra we need to scale the diffusivity approximately as a power law of the model truncation (the regression fit shown in Figure 3 is $1.2 \times 10^{21} n_t^{-3.22} \text{ m}^4 \text{ s}^{-1}$, where n_t is the truncation wavenumber). Also shown are results for the recommended diffusivity values for T21, T31, T42 and T63 determined by *Boville* [1991] in a similar manner using a different spectral GCM.

[11] The dashed line in Figure 3 shows spectra computed from a T639 integration identical in all respects to the control run, but employing twice the vertical resolution (T639L48). The result is reasonably close to that from the 24-level version, although there seems to be a systematic difference between $n \sim 10$ and $n \sim 50$ where the L48 model has more KE than the L24 version.

5. Results for Dry Dynamical Core Model

[12] If KH are correct and the energy in the mesoscale is at least partly due to downscale spectral cascades from the synoptic scales, then a shallow mesoscale spectrum may be expected even in a model with no moist convection. In order to test this notion, we constructed a dry dynamical core

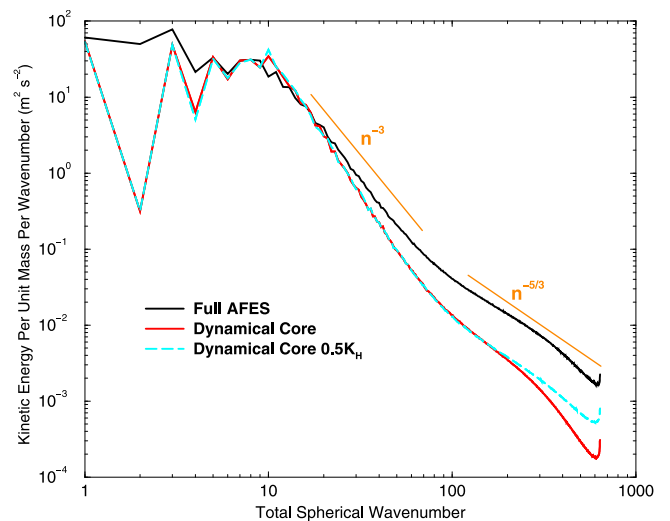


Figure 4. As in Figure 2, but for the control T639L24 AFES (black) and the dynamical core version of the model run with the same horizontal diffusion coefficient as employed in the standard AFES (red) and with half this diffusion coefficient (blue).

(DDC) version of the AFES model following Held and Suarez [1994, hereinafter referred to as HS]. This version has no topography, no latent heat release and has the radiative code replaced by a simple relaxation toward a specified radiative state. The choices of radiative state and relaxation rates follow those of HS, and are designed to simulate a tropospheric zonal-mean state that at least roughly approximates the observed annual-mean state. The DDC model was integrated at T639L24 resolution for 15 days from initial conditions interpolated from the end of a long run of a T319L24 version. The red curve in Figure 4 shows the 2D KE spectrum at 200 hPa calculated from the last 10 days of the DDC integration, the blue curve shows the same quantity from a DDC run with 1/2 the standard diffusivity. Also shown is the result from the standard full AFES model. The HS radiative terms have produced a simulation with KE in the baroclinically unstable scales very similar to that in the full model. The DDC model (with no topography) not surprisingly has much less KE at very small wavenumbers. In the mesoscale both versions of the DDC model simulate a clear shallow mesoscale spectrum for n greater than about 80. Just as in the full model, the spectrum for about $n > 300$ is strongly dependent on the diffusivity employed, but the break in power law behavior at the beginning of the mesoscale seems to be reasonably independent of the diffusivity coefficient. The energy in the mesoscale in the DDC model is only about 1/4 of that in the full AFES model. This result would seem to be in agreement with the earlier determination by KH that the mesoscale in a full GCM is energized by both forward spectral cascades (still present in the DDC model) and moist convective forcing (absent from the DDC model).

6. Conclusion

[13] The present results confirm the earlier finding of KH that a global GCM run in control mode can spontaneously simulate a realistic KE spectrum through a decade or more of the mesoscale. It is noteworthy that SKYHI and AFES produce comparable simulations of the KE spectrum despite the rather different formulations of the SKYHI model (notably A-grid horizontal differencing and the use of MCA) and AFES (spectral representation in the horizontal and Emanuel moist convection parameterization). It is known, however, that at least one other current GCM does not produce a realistically shallow KE spectrum in the mesoscale [Palmer, 2001]. It is interesting to note that, despite their differences, AFES and SKYHI both avoid semi-lagrangian or other upstream differencing approximations in their numerical formulation. So it may be that models that have fundamentally dissipation-free numerics (and thus have small scale dissipation controlled by the explicitly parameterized subgrid-scale diffusion) are able to simulate a realistic mesoscale. Our results also lead to a prescription for scaling the hyperdiffusion coefficient with model resolution in atmospheric GCMs.

[14] The present DDC experiments show explicitly that a global model without latent heating can produce a shallow mesoscale, confirming the notion that the mesoscale is energized by downscale nonlinear spectral cascades. However, the comparison of the results in the DDC model and the full AFES suggests that moist convective processes also

contribute significantly to the excitation of the mesoscale kinetic energy. However, even the rather fine resolution AFES GCM is far from including an explicit representation of moist convection, and it is possible that the forcing of the mesoscale by convection in the real world could differ significantly from that seen in the model.

[15] **Acknowledgments.** This work was supported by NSF Award ATM02-19120 and by JAMSTEC through its sponsorship of the International Pacific Research Center. This research was partly supported by the Research Fellowships for Young Scientists of the Japan Society for the Promotion of Science. The calculations were performed on the JAMSTEC Earth Simulator.

References

- Arakawa, A. (1966), Computational design for long-term numerical integrations of the equations of atmospheric motion, *J. Comput. Phys.*, *1*, 119–143.
- Boer, G. J., and T. G. Shepherd (1983), Large-scale two-dimensional turbulence in the atmosphere, *J. Atmos. Sci.*, *40*, 164–184.
- Boville, B. A. (1991), Sensitivity of simulated climate to model resolution, *J. Clim.*, *4*(5), 469–485, doi:10.1175/1520-0442(1991)004<0469:SOSCTM>2.0.CO;2.
- Cho, J. Y. N., et al. (1999a), Horizontal wavenumber spectra of winds, temperature, and trace gases during the Pacific Exploratory Missions: 1. Climatology, *J. Geophys. Res.*, *104*, 5697–5716.
- Cho, J. Y. N., R. E. Newell, and J. D. Barrick (1999b), Horizontal wavenumber spectra of winds, temperature, and trace gases during the Pacific Exploratory Missions: 2. Gravity waves, quasi-two-dimensional turbulence, and vortical modes, *J. Geophys. Res.*, *104*, 16,297–16,308.
- Emanuel, K. A. (1991), A scheme for representing cumulus convection in large-scale models, *J. Atmos. Sci.*, *48*, 2313–2335.
- Gage, K. S., and G. D. Nastrom (1986), Theoretical interpretation of atmospheric wavenumber spectra of wind and temperature observed by commercial aircraft during GASP, *J. Atmos. Sci.*, *43*, 729–740.
- Held, I. M., and M. J. Suarez (1994), A proposal for the intercomparison of dynamical cores of atmospheric general circulation models, *Bull. Am. Meteorol. Soc.*, *75*, 1825–1830.
- Koshyk, J. N., and K. Hamilton (2001), The horizontal kinetic energy spectrum and spectral budget simulated by a high-resolution troposphere-stratosphere-mesosphere GCM, *J. Atmos. Sci.*, *58*, 329–348.
- Koshyk, J. N., B. Boville, K. Hamilton, E. Manzini, and K. Shibata (1999), The kinetic energy spectrum of horizontal motions in middle-atmosphere models, *J. Geophys. Res.*, *104*, 27,177–27,190.
- Lander, J., and B. J. Hoskins (1997), Believable scales and parameterizations in a spectral model, *Mon. Weather Rev.*, *125*, 292–303.
- Lilly, D. (1983), Stratified turbulence and the mesoscale variability of the atmosphere, *J. Atmos. Sci.*, *40*, 749–761.
- Lindborg, E. (1999), Can the atmospheric kinetic energy spectrum be explained by two-dimensional turbulence?, *J. Fluid Mech.*, *388*, 259–288.
- Nastrom, G. D., and K. S. Gage (1985), A climatology of atmospheric wavenumber spectra of wind and temperature observed by commercial aircraft, *J. Atmos. Sci.*, *42*, 950–960.
- Numaguti, A., et al. (1997), Study on the climate system and mass transport by a climate model, *CGER's Supercomputer Monograph*, vol. 3, Cent. for Global Environ. Res., Natl. Inst. for Environ. Stud., Tsukuba, Japan.
- Ohfuchi, W., et al. (2004), 10-km mesh meso-scale resolving simulations of the global atmosphere on the Earth Simulator—Preliminary outcomes of AFES, *J. Earth Simulator*, *1*, 8–34.
- Palmer, T. N. (2001), A nonlinear dynamical perspective on model error: A proposal for non-local stochastic-dynamic parameterization in weather and climate prediction models, *Q. J. R. Meteorol. Soc.*, *127*, 279–304.
- Vallis, G. K., G. J. Shutts, and M. E. B. Gray (1997), Balanced mesoscale motion and stratified turbulence forced by convection, *Q. J. R. Meteorol. Soc.*, *123*, 1621–1652.
- VanZandt, T. E. (1982), A universal spectrum of buoyancy waves in the atmosphere, *Geophys. Res. Lett.*, *9*, 575–578.
- Yuan, L., and K. Hamilton (1994), Equilibrium dynamics in a forced-dissipative f-plane shallow water model, *J. Fluid Mech.*, *280*, 369–394.

K. Hamilton, International Pacific Research Center, University of Hawaii, Honolulu, HI 96822, USA. (kph@hawaii.edu)

W. Ohfuchi, Earth Simulator Center, Japan Agency for Marine-Earth Science and Technology, Yokohama 236-0001, Japan.

Y. O. Takahashi, Graduate School of Science, Hokkaido University, Sapporo 060-0808, Japan.